THE ASTROPHYSICAL JOURNAL, 562:L163–L166, 2001 December 1
© 2001. The American Astronomical Society. All rights reserved. Printed in U.S.A.

X-RAY DETECTION OF PULSAR PSR B1757−24 AND ITS NEBULAR TAIL

V. M. KASPI,[1,2,3] E. V. GOTTHELF,[4] B. M. GAENSLER,[2,5] AND M. LYUTIKOV[1,6]

Received 2001 August 9; accepted 2001 October 4; published 2001 November 14

ABSTRACT

We report the first X-ray detection of the radio pulsar PSR B1757−24 using the *Chandra X-Ray Observatory*. We detect point-source emission at the pulsar position plus a faint tail extending nearly 20″ east of the pulsar, in the same direction and with comparable morphology to the radio tail. Assuming the point-source X-ray emission is magnetospheric, the observed X-ray tail represents only ∼0.01% of the pulsar's spin-down luminosity. This is significantly lower than the analogous efficiencies of most known X-ray nebulae surrounding rotation-powered pulsars. Assuming a nonthermal spectrum for the tail photons, we show that the tail is unlikely to be emission left behind following the passage of the pulsar but rather is probably from synchrotron-emitting pulsar wind particles having a flow velocity of ∼7000 km s^{-1}. We also show that there must be a significant break in the tail synchrotron spectrum between the radio and X-ray bands that is intrinsic to the particle spectrum. No emission is detected from the shell supernova remnant G5.4−1.2. The upper limits on remnant emission are unconstraining.

Subject headings: ISM: individual (G5.4−1.2) — pulsars: general — pulsars: individual (PSR B1757−24) — X-rays: general

1. INTRODUCTION

PSR B1757−24 is a 124 ms radio pulsar discovered near the supernova remnant (SNR) G5.4−1.2 (Manchester et al. 1985). Radio timing observations established that the pulsar has a characteristic age of 16 kyr and spin-down luminosity $\dot{E} = 2.6 \times 10^{36}$ ergs s^{-1} (Manchester et al. 1991). The pulsar is at the tip of a flat-spectrum radio protuberance just outside the west side of the SNR shell. The protuberance consists of a small, roughly circular nebula, G5.27−0.90, from which a collimated jetlike feature is emerging on its western side. The pulsar is at the westernmost tip of the collimated feature. The morphology and spectrum of the jet are strongly suggestive of a ram-pressure–confined pulsar wind nebula (PWN; Frail & Kulkarni 1991). Thus, assuming an association between the pulsar and G5.4−1.2, the former appears to have overtaken the expanding shell, presumably because of a large kick at birth. Given the angular displacement of the pulsar from the best-estimate remnant center, and if the pulsar's characteristic age is a good estimate of its true age, this implies a proper motion of ∼75 mas yr^{-1}, corresponding to a transverse space velocity of $v_t \sim 1800$ km s^{-1} (Frail, Kassim, & Weiler 1994), for a distance of 5 kpc (Caswell et al. 1987; Frail et al. 1994). However, recent interferometric observations have failed to detect the implied proper motion (Gaensler & Frail 2000). They set a 5 σ upper limit on the proper motion of less than 25 mas yr^{-1}, corresponding to $v_t < 590$ km s^{-1}. This suggests that the pulsar is older than its characteristic age or that the assumed pulsar birth place is incorrect.

A ram-pressure–confined pulsar wind should radiate X-rays as part of the broadband synchrotron spectrum that results from the shock acceleration and subsequent gyration of relativistic wind electron/positron pairs in the ambient magnetic field. We report here on *Chandra X-Ray Observatory* observations of PSR B1757−24 in which we detect the source for the first time in X-rays.

2. OBSERVATIONS AND RESULTS

The PSR B1757−24/G5.4−1.2 field was observed using the Advanced CCD Imaging Spectrometer (ACIS) instrument aboard the *Chandra X-Ray Observatory* on 2000 April 12. The ACIS CCD camera (Burke et al. 1997) is sensitive to X-rays in the 0.2–10 keV band with 0.″492 pixels. The pulsar was positioned on the back-illuminated S3 chip of the ACIS-S array, offset from the aim point by −0.″37 in the *Y*-direction, in order to avoid source counts from being split between two readout nodes. Data were collected in the nominal timing mode, with 3.241 s exposures between CCD readouts, and "FAINT" spectral mode. The standard *Chandra* screening criteria produced a total usable exposure time of 19.6 ks.

The ACIS image reveals a faint point source near the radio pulsar position and a fainter tail of emission on the eastern side, similar to the radio emission (Fig. 1). Figure 2 shows the distribution of counts as a function of distance from the point source (with the point source excluded) in two 30° wedges on the eastern and western sides of the pulsar, along with the mean of the field. With respect to the mean and the western side, the eastern side clearly has an overdensity of counts extending nearly 20″ from the point source. Simulations of a point source at the pulsar position using the *Chandra* simulator MARX are consistent with what is observed in all directions but east. As the tail is in the chip readout direction, we were concerned about it being an instrumental artifact. However, trails in ACIS images aligned with the readout direction are seen only for bright sources, are symmetric about them, and have uniform intensity along the readout axis (M. Bautz, D. Edgar, & H. Marshall 2001, private communication). Furthermore, we verified that there were no pointing anomalies during the observation and that the count rate for the tail photons is uniform in time over the observation. We therefore conclude that the extended, collimated emission we have detected is genuinely astrophysical.

The standard processing for ACIS produces measured source

[1] Department of Physics, Rutherford Physics Building, McGill University, 3600 University Street, Montreal, QC H3A 2T8, Canada.
[2] Department of Physics and Center for Space Research, Massachusetts Institute of Technology, Cambridge, MA 02139.
[3] Canada Research Chair, Alfred P. Sloan Fellow.
[4] Astronomy Department, Columbia University, Pupin Hall, 550 West 120th Street, New York, NY 10027.
[5] Hubble Fellow. Current address: Harvard-Smithsonian Center for Astrophysics, 60 Garden Street, Cambridge, MA 02138.
[6] CITA National Fellow.

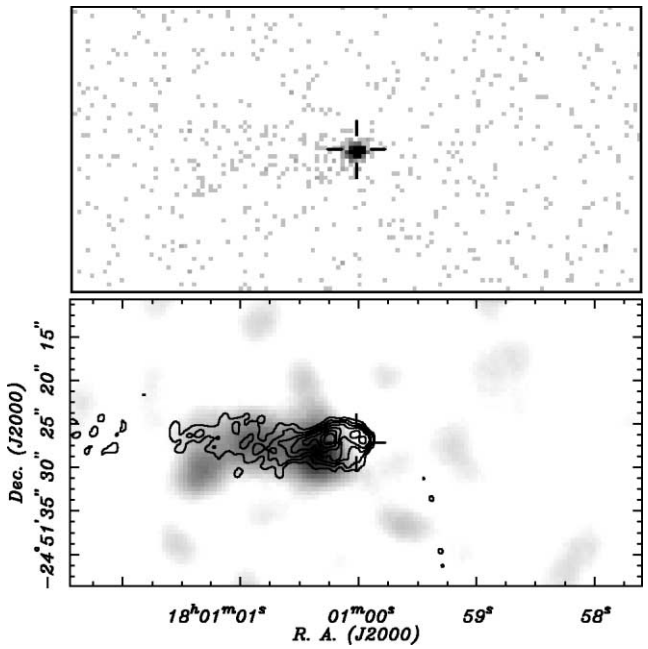


FIG. 1.—*Chandra* X-ray detection of PSR B1757−24 and its nebular tail. *Top panel*: Gray-scale plot of the 0.3–10 keV image, centered on the pulsar, and scaled to show all pixels with detected photons. The X-ray point source is coincident with the radio pulsar position, denoted by the cross. The contours show 4.9 GHz emission in equally spaced contours ranging from 0.17 to 0.56 mJy beam^{-1}. The radio data have beam size 1.″2 and were obtained at the VLA on 1999 October 23 by one of us (B. Gaensler). *Bottom panel*: Same image with the X-ray point-source contribution removed, the image smoothed with a Gaussian of width ∼2″, and the intensity scaled to emphasize the diffuse X-ray emission.

coordinates with a nominal accuracy quoted as 0.″6; however, several problems are known to exist with the plate scale solution at the time of writing.[7] We derived our own astrometric solution by comparing field stars in our observation with cataloged optical coordinates. The X-ray source positions were measured using the CIAO source detection software CELLDETECT with the cleaned 0.3–10 keV level 2 event file as input. For a signal-to-noise ratio threshold set to 3 and the background estimated using LDETECT, we found nine significant X-ray sources within 5′ of the pulsar position. The on-line USNO-A2.0 astrometric reference catalogs (Monet et al. 1996) provided likely counterparts for eight of the nine X-ray sources. The USNO catalog gives stellar positions to a nominal 1 σ error of ≈0.″25 (Deutsch 1999; D. Monet 2001, private communication), although proper motion has not been applied. The offsets between the optical and X-ray positions are well clustered, strongly suggesting correct identifications. The average offset is ∼0.″6, consistent with the expected systematic error in the absolute coordinates of ACIS. The calibrated position of the putative X-ray counterpart to the pulsar is R.A. = $18^{h}01^{m}00\overset{s}{.}027$, decl. = −24°51′27.″53 (J2000.0) with rms error 0.″31. This is within 1.2 σ of the radio pulsar location found by Gaensler & Frail (2000). Thus, the point source is consistent with being the X-ray counterpart of the pulsar.

To characterize the energy dependence of the emission from the point source, a spectrum was extracted from a circular region having radius 7 pixels (3.″4). An annular background region was chosen (approximately centered on the point source) having inner and outer radii of 33 and 98 pixels, respectively.

[7] See http://asc.harvard.edu/mta/ASPECT/aspect_caveats.html.

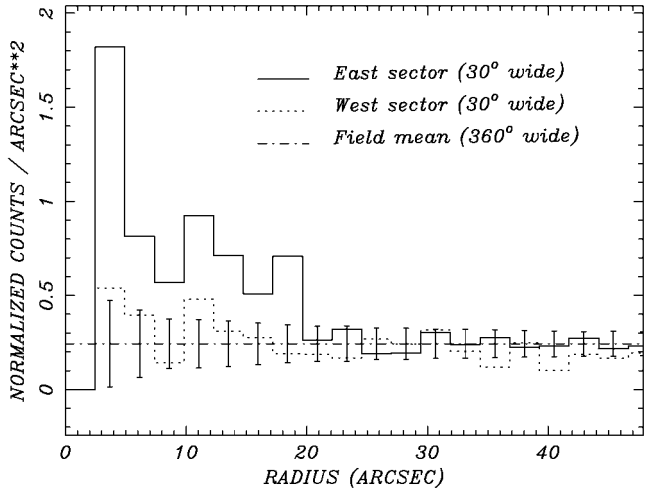


FIG. 2.—X-ray intensity as a function of radius from the point source in two 30° wedges, one east (*solid line*) and one west (*dotted line*) of the pulsar. The point-source emission has been subtracted from the plot. The field mean is shown by a dot-dashed line. 1 σ error bars for each radial bin are shown.

We found a total of 438 source counts and an estimated eight background counts in the source region. We note that the background on the S3 chip was dominated by scattered emission from the nearby bright X-ray binary GX 5−1. The CIAO tools MKRMF and MKARF were used to generate common response files for the source and background regions. The data were regrouped such that spectral bins contained a minimum of 15 counts, resulting in 27 independent spectral bins. We fitted the spectrum with the spectral analysis package XSPEC (version 11). We characterize the spectrum using two different models: a power law and thermal bremsstrahlung, each photoelectrically absorbed. Both provide acceptable fits, although the plasma temperature in the thermal model is poorly constrained. The results are shown in Table 1. We verified using XSPEC that the expected ∼2.6% pileup fraction does not have a significant impact on the fitted parameters.

The tail east of the pulsar is much fainter than the point source. We attempted to characterize its spectrum by assuming a power-law model and holding the equivalent neutral hydrogen column density $N_{\rm H}$ fixed at the value determined from the point source (see Table 1). We extracted a spectrum for the tail using a box having dimensions 40 × 18 pixels, which contained 118 counts. We used the same annulus to estimate the background as we did for the point source; in this way we estimate that approximately 40 counts were from the background, leaving 78 source counts. Spectral fits to the tail in the 0.3–9 keV range for a power-law model yielded a mediocre fit to the data (χ^2_ν = 2.0 for 4 degrees

TABLE 1

SPECTRAL PARAMETERS FOR PSR B1757−24 FOR TWO TRIAL MODELS

Parameter	Power Law	Thermal Bremsstrahlung
$N_{\rm H}$ (10^{22} cm^{-2})	$3.5^{+1.3}_{-1.1}$	$3.3^{+0.76}_{-1.0}$
Γ[a]	$1.6^{+0.6}_{-0.5}$	...
kT (keV)	...	$16^{+\infty}_{-8}$
Absorbed flux[b]	$5.4^{+0.4}_{-0.5}$	$5.1^{+0.4}_{-0.5}$
Unabsorbed flux[b]	$6.9^{+0.5}_{-0.6}$	$6.6^{+0.5}_{-0.6}$
χ^2_ν (for 24 dof)	1.24	1.26

NOTE.—Uncertainties reported are at the 90% confidence level.
[a] Photon index.
[b] In units of 10^{-13} ergs cm^{-2} s^{-1} in the 2–10 keV band.

of freedom [dof]). The best-fit power-law photon index of 1.0 ± 0.6 is consistent with relatively hard emission, as implied by the existence of a significant number of counts above 5 keV. However, given the 90% confidence range for $N_{\rm H}$ (Table 1), we found that photon indexes in the range from -0.32 to 1.8 are consistent with the data. Lower values of $N_{\rm H}$, corresponding to lower values of the photon index, give slightly better fits. Improved characterization of the spectrum of the tail must await a deeper observation of the source. Nevertheless, we can determine the absorbed surface brightness in the 2–8 keV band to be 4.5×10^{-16} ergs s^{-1} cm^{-2} arcsec^{-2}, with uncertainty of ~30%. The total unabsorbed flux in the 2–8 keV band in our extraction region is 9.8×10^{-14} ergs s^{-1} cm^{-2}, with similar uncertainty.

3. DISCUSSION

3.1. *The Pulsar*

Given the spatial coincidence of the X-ray point source with the radio pulsar position, the former is likely to be emission from the radio pulsar itself, in particular, nonthermal pulse-phase–averaged magnetospheric emission. The observed 2–10 keV flux (Table 1) implies an unabsorbed luminosity, for a distance $d = 5$ kpc, of 2×10^{33} ergs s^{-1}, assuming beaming angle $\phi = \pi$ sr. This implies an efficiency of conversion of spin-down luminosity into magnetospheric emission of $0.00020(\phi/\pi \text{ sr})(d/5 \text{ kpc})^2$. This efficiency, as well as the measured power-law photon index (Table 1), are consistent with those observed for the magnetospheric components of other radio pulsars (Becker & Trümper 1997). The detection of low duty cycle X-ray pulsations could unambiguously confirm this interpretation. The current data cannot however rule out the possibility that the emission is coming from a very compact nebular region near the pulsar. At radio wavelengths, the head of the bow shock is only ~1.″5 from the pulsar (Gaensler & Frail 2000). The reverse shock, which terminates the wind, is likely unresolvable in the *Chandra* image.

Marsden, Lingenfelter, & Rothschild (2001) suggested that PSR B1757−24 has a fallback disk from which it accretes, providing nonmagnetic dipole spin-down torque to account for the possible difference between the pulsar's true and characteristic ages. They predict a thermal bremsstrahlung spectrum having $kT \sim 50$ keV and an X-ray luminosity (in an unspecified energy band) roughly an order of magnitude less than that predicted for magnetospheric emission. The *Chandra* detection we report here is consistent with standard magnetospheric emission. However, our data cannot rule out a fainter thermal component.

3.2. *The Nebular Tail*

The tail X-ray emission is likely to be synchrotron radiation from the shocked pulsar wind. The pulsar wind appears to be confined by the ram pressure of the interstellar medium. If the pulsar's space velocity greatly exceeds the ambient medium's sound speed, a strong forward bow shock travels in front of it, and a reverse shock closer to the pulsar terminates its relativistic wind.

Conventional wisdom suggests that X-ray synchrotron nebulae should be smaller than the corresponding radio nebulae because radio electrons have much longer lives than do X-rays. This is consistent with the apparent contraction of the Crab Nebula with increasing photon energy. However, for PSR B1757−24, Figures 1 and 2 demonstrate that the observed X-ray tail extends nearly 20″ [0.48(d/5 kpc) pc] to the east of the pulsar, nearly as long as the detected radio tail (which, ~10″ further east, suddenly expands to form the flat-spectrum bubble, G5.27−0.90; Frail & Kulkarni 1991). The 5 σ upper limit on the proper motion implies a transverse velocity of $v_t < 590$ km s^{-1} (Gaensler & Frail 2000). Thus, the time since the pulsar was at the easternmost tip of the observed X-ray emission must be greater than 800 yr. The synchrotron lifetime of a photon of energy E (in keV) in a magnetic field B_{-4} (in units of 10^{-4} G) is $t_s \simeq 40E^{-1/2}B_{-4}^{-3/2}$ yr. Thus, for $t_s > 800$ yr and $E \simeq 1$–9 keV, $B < 0.8$–14 μG. This is much less than the equipartition magnetic field $B_{\rm eq} \sim (\dot{E}/r_s^2 c)^{1/2} \sim 70$ μG expected in the vicinity of the pulsar. Here, r_s is the distance from the pulsar to the bow shock head, the approximate scale over which equipartition should hold (Kennel & Coroniti 1984). This assumes the flow is subsonic, being confined on the trailing side by the high SNR pressure. This assumption seems reasonable, as in the absence of such confinement, it is hard to understand why this pulsar, which has space velocity not much larger than the average pulsar (e.g., Lyne & Lorimer 1994), should have such a striking ram-pressure–confined PWN. Hence, the X-ray tail behind PSR B1757−24 is unlikely to be a trail in the conventional sense, in that it cannot be synchrotron emission from pulsar wind particles just left behind after the passage of the pulsar.

Rather, assuming the spectrum of the tail is indeed nonthermal, freshly shocked wind particles must be continuously fed eastward with a velocity much larger than the pulsar space velocity, $v_f \gg v_t$. This is similar to the picture suggested for a putative X-ray tail behind PSR B1929+10 (see Wang, Li, & Begelman 1993, although that tail has not been confirmed) and a cometary-shaped PWN in the LMC SNR N157B (Wang & Gotthelf 1998). However, M. Lyutikov (2001, in preparation) has developed an alternative model of the structure of the tail region. In this model, the pulsar wind is shocked near the pulsar and forms a subsonically expanding tail confined by interstellar medium ram pressure (without forming a de Laval nozzle as suggested by Wang et al. 1993). The typical velocities of the flow are weakly relativistic near the pulsar, decreasing downstream as the tail expands. At its end, the tail flow finally forms a pressure-confined expanding bubble, presumably G5.27−0.90.

We can constrain the flow velocity v_f of the wind particles in the tail by noting that it must be high enough to continuously supply particles given their cooling times. Thus, the flow time $t_f \lesssim t_s$. Assuming that the magnetic field reaches its equipartition value near the bow shock head and that this value holds for the approximately one-dimensional tail region too, we find $t_s \gtrsim 70(E/1 \text{ keV})^{-1/2}(B_{\rm eq}/70 \ \mu\text{G})^{-3/2}$ yr. As the tail extends to 0.48 pc for $d = 5$ kpc, this implies $v_f \gtrsim 6800 \times (d/5 \text{ kpc})(E/1 \text{ keV})^{1/2}(B_{\rm eq}/70 \ \mu\text{G})^{3/2}$ km s^{-1}.

The tail emission has low flux. The efficiency with which the pulsar's $\dot{E}$ is converted into tail X-rays in the 2–8 keV band is only $0.00011(d/5 \text{ kpc})^2$, roughly half of the point-source efficiency. This is in contrast to other rotation-powered pulsars, like the Crab, whose X-ray nebular emission is much brighter than the point-source output. Without timing information, we cannot rule out an ultracompact nebula as the source of the point-source emission. But even so, the total efficiency for conversion of spin-down energy to nebula energy would be significantly less than that of most rotation-powered pulsars (Becker & Trümper 1997).

Several effects may reduce the X-ray efficiency of ram-pressure–confined PWNs. First, the efficiency of conversion of E into X-ray–emitting particles may be lower since the reverse shock in the ram-pressure–confined PWNs is strong only in

the forward part of the head, subtending a much smaller solid angle than in a static PWN. Second, the low X-ray efficiency is expected if the flow time of the relativistic plasma through the tail is shorter than the synchrotron lifetime. In this case the particles will be able to emit only a small fraction of the energy that they acquired during acceleration at the reverse shock; most of the energy of the wind will be spent on doing work inflating the bubble at the end of the tail. Indeed, a similar argument was put forth by Chevalier (2000) to explain the low efficiencies of the Vela and CTB 80 pulsars, both of which exhibit bow shock morphologies and have relatively flat spectra. Finally, it is also possible that low surface brightness emission from beyond the eastern tip of the observable X-ray tail, or even from G5.27−0.90, has gone undetected in our observation. For example, emission from the direction of that nebula, having X-ray surface brightness half of the ACIS-S3 background, would contribute roughly 2 orders of magnitude more flux.

We can compare the observed X-ray tail flux with that predicted from the radio flux density and spectrum. Frail & Kulkarni (1991) found that the radio tail has a flat spectrum ($\alpha \simeq 0$, where α is the energy spectral index), consistent with what we find at X-ray energies (§ 2). However, it is impossible to produce a continuous spectrum for the tail between the radio, where $f_{20\,\mu\mathrm{eV}} = 2.4 \times 10^{-8}$ ergs cm^{-2} s^{-1} keV^{-1} (Frail & Kulkarni 1991), and X-ray bands, where $f_{5\,\mathrm{keV}} \approx 1.6 \times 10^{-14}$ ergs cm^{-2} s^{-1} keV^{-1} (§ 2). Thus there must be an intrinsic spectral break, which, even if it lies as low as in the radio band (e.g., 5 GHz), demands an X-ray photon index greater than 1.8, much larger than expected for a synchrotron cooling break, and only marginally consistent with the data (§ 2). Therefore, the broadband spectrum has at least two inflection points between the radio and X-ray bands; i.e., the emission in the two bands originates from separate populations of accelerated particles. The same problem arises in the Crab Nebula (e.g., see Kennel & Coroniti 1984).

4. THE SUPERNOVA REMNANT

We have detected no X-ray emission from SNR G5.4−1.2. Assuming an association, if the pulsar's characteristic age is a good estimate of the true age, then the SNR is young ($t_{\mathrm{SNR}} \sim 16$ kyr), and we might expect thermal X-ray emission from hot gas behind the SNR shock. We considered a $4' \times 4'$ region of the SNR centered on coordinates R.A. $= 18^{\mathrm{h}}01^{\mathrm{m}}18^{\mathrm{s}}$, decl. $= -24°51'10''$ (J2000.0). A background correction was applied using a region having the same dimensions next to the source region, scaling for the different effective areas. We find no excess emission in this region, with a 5 σ upper limit on the count rate of 0.017 counts s^{-1} in the range 0.3–8.0 keV. Assuming $d = 5$ kpc, the shock velocity in the Sedov solution should be ~600 km s^{-1}, corresponding to a shock temperature $kT \approx 0.5$ keV. Using a Raymond-Smith model with $kT = 0.5$ keV and $N_{\mathrm{H}} = 3 \times 10^{22}$ cm^{-2} and assuming the area under consideration encloses a volume of $\sim 6 \times 10^{57}$ cm^3, the limit on the count rate in this region corresponds to $n_e n_{\mathrm{H}} < 0.15$ cm^{-6}, where n_e and n_{H} are the electron and hydrogen densities, respectively. Assuming a composition of pure ionized hydrogen, the upper limit on the preshock density is $n_{\mathrm{H}} < 0.1$ cm^{-3}. This result is not a strong function of the assumed temperature: for $kT = 0.2$ (5) keV, we find $n_{\mathrm{H}} < 0.50$ (0.04) cm^{-3}. These limits are unconstraining. If the system has an age of 16 kyr, the inferred density is $n_{\mathrm{H}} \sim 0.003$ cm^{-3} (Frail & Kulkarni 1991). If the SNR is much older than indicated by the pulsar's spin-down (Gaensler & Frail 2000), then the SNR expansion speed is less than 100 km s^{-1} and any X-ray emission from the SNR is expected to be too faint to detect for this distance and absorption.

We thank M. Roberts for useful discussions. This work is supported by SAO grant GO0-1133A, NASA LTSA grant NAG5-8063, and NSERC grant RGPIN 228738-00 to V. M. K. E. V. G. is supported by the NASA LTSA grant NAG5-22250. B. M. G. acknowledges the support of a Hubble Fellowship awarded by STScI.

REFERENCES

Becker, W., & Trümper, J. 1997, A&A, 326, 682
Burke, B. E., Gregory, J., Bautz, M. W., Prigozhin, G. Y., Kissel, S. E., Kosicki, B. N., Loomis, A. H., & Young, D. J. 1997, IEEE Trans. Electron. Devices, 44, 1633
Caswell, J. L., Kesteven, M. J., Komesaroff, M. M., Haynes, R. F., Milne, D. K., Stewart, R. T., & Wilson, S. G. 1987, MNRAS, 225, 329
Chevalier, R. A. 2000, ApJ, 539, L45
Deutsch, E. W. 1999, AJ, 118, 1882
Frail, D. A., Kassim, N. E., & Weiler, K. W. 1994, AJ, 107, 1120
Frail, D. A., & Kulkarni, S. R. 1991, Nature, 352, 785
Gaensler, B. M., & Frail, D. A. 2000, Nature, 406, 158
Kennel, C. F., & Coroniti, F. V. 1984, ApJ, 283, 710
Lyne, A. G., & Lorimer, D. R. 1994, Nature, 369, 127
Manchester, R. N., D'Amico, N., & Tuohy, I. R. 1985, MNRAS, 212, 975
Manchester, R. N., Kaspi, V. M., Johnston, S., Lyne, A. G., & D'Amico, N. 1991, MNRAS, 253, 7P
Marsden, D., Lingenfelter, R. E., & Rothschild, R. E. 2001, ApJ, 547, L45
Monet, D., et al. 1996, USNO-SA2.0 (Washington, DC: USNO)
Wang, Q. D., & Gotthelf, E. V. 1998, ApJ, 494, 623
Wang, Q. D., Li, Z.-Y., & Begelman, M. C. 1993, Nature, 364, 127